



Generation and Characterization of a Novel Mouse Model That Allows Spatiotemporal Quantification of Pancreatic β -Cell Proliferation

Shinsuke Tokumoto,¹ Daisuke Yabe,^{1,2} Hisato Tatsuoka,¹ Ryota Usui,¹ Muhammad Fauzi,¹ Ainur Botagarova,¹ Hisanori Goto,¹ Pedro Luis Herrera,³ Masahito Ogura,¹ and Nobuya Inagaki¹

Diabetes 2020;69:2340–2351 | <https://doi.org/10.2337/db20-0290>

Pancreatic β -cell proliferation has been gaining much attention as a therapeutic target for the prevention and treatment of diabetes. In order to evaluate potential β -cell mitogens, accurate and reliable methods for the detection and quantification of the β -cell proliferation rate are indispensable. In this study, we developed a novel tool that specifically labels replicating β -cells as mVenus⁺ cells by using RIP-Cre; R26Fucci2aR mice expressing the fluorescent ubiquitination-based cell cycle indicator Fucci2a in β -cells. In response to β -cell proliferation stimuli, such as insulin receptor antagonist S961 and diet-induced obesity (DIO), the number of 5-ethynyl-2'-deoxyuridine-positive insulin⁺ cells per insulin⁺ cells and the number of mVenus⁺ cells per mCherry⁺ mVenus⁻ cells + mCherry⁻ mVenus⁺ cells were similarly increased in these mice. Three-dimensional imaging of optically cleared pancreas tissue from these mice enabled quantification of replicating β -cells in the islets and morphometric analysis of the islets after known mitogenic interventions such as S961, DIO, pregnancy, and partial pancreatectomy. Thus, this novel mouse line is a powerful tool for spatiotemporal analysis and quantification of β -cell proliferation in response to mitogenic stimulation.

Diabetes is caused by β -cell dysfunction as well as increased insulin resistance. Stimulation of β -cell proliferation is therefore a promising strategy for the prevention and treatment of diabetes. In an attempt to evaluate potential β -cell mitogens, accurate and reliable methods

for the detection and quantification of β -cell proliferation are indispensable. So far, determination of the β -cell proliferation rate has relied on immunohistochemical detection of cell cycle markers such as nucleotide analogs (BrdU and 5-ethynyl-2'-deoxyuridine [EdU]) or replication proteins (proliferating cell nuclear antigen and Ki-67). However, the β -cell proliferation rates obtained by immunohistochemical analysis are not always accurate and reproducible (1,2), and methodological differences in immunolabeling and image acquisition techniques can cause interlaboratory variability of results (2). In addition, three-dimensional (3D) analysis of whole islets has not been possible, and replicating non- β -cells overlying quiescent β -cells within islets can confound results. Furthermore, the sampling size of β -cells is sometimes inadequate because the data are acquired from a certain number of pancreatic sections per condition. Thus, a new method for quantifying replicating β -cells that compensates for these limitations is required.

The fluorescent ubiquitination-based cell cycle indicator (Fucci) reporter is a well-established probe for monitoring cell cycle status (3). The Fucci system relies on the expression of a pair of fluorescent proteins: mCherry-hCdt1 (30/120) (a fragment with degradation sequence [degron] of chromatin licensing and DNA replication factor [Cdt]1 fused to a fluorescent protein in the red spectrum) and mVenus-hGem (1/110) (a degron of Geminin fused to a fluorescent protein in the green spectrum). Reciprocal expression of these paired proteins labels cells in the G₁ phase and those in the S/G₂/M phase with red and green

¹Department of Diabetes, Endocrinology and Nutrition, Graduate School of Medicine, Kyoto University, Kyoto, Japan

²Department of Diabetes and Endocrinology, Gifu University Graduate School of Medicine, Gifu, Japan

³Department of Genetic Medicine and Development, University of Geneva Medical School, Geneva, Switzerland

Corresponding author: Nobuya Inagaki, inagaki@kuhp.kyoto-u.ac.jp

Received 24 March 2020 and accepted 2 August 2020

This article contains supplementary material online at <https://doi.org/10.2337/figshare.12753533>.

© 2020 by the American Diabetes Association. Readers may use this article as long as the work is properly cited, the use is educational and not for profit, and the work is not altered. More information is available at <https://www.diabetesjournals.org/content/license>.

fluorescence, respectively. Thus, the Fucci system can be used to visualize the G₁/S transition and thus quantify replicating β -cells.

In this study, we generated and characterized a mouse line in which the Fucci probe is expressed in β -cells to monitor their cell cycle phase. Using this model, we evaluated β -cell proliferation induced by administration of the insulin receptor antagonist S961, a reported β -cell mitogen (4), diet-induced obesity (DIO) (5), pregnancy (6,7) and partial pancreatectomy (PPTX) (8). In addition, we performed 3D analyses of whole islets by observing optically cleared pancreata of these mice and found a strong and significant correlation between islet size and the number of replicating β -cells per islet. These results demonstrate the usefulness of this mouse model for the study of β -cell proliferation.

RESEARCH DESIGN AND METHODS

Animals

To establish the mouse model for studying β -cell proliferation, we used R26Fucci2aR mice in which a single copy of the Fucci2a transgene under the control of the cytomegalovirus early enhancer/chicken β -actin promoter was inserted into the Rosa26 locus by homologous recombination (RIKEN BRC06511) (9). This newer Fucci2a reporter is a bicistronic Cre-inducible probe consisting of two fluorescent proteins: truncated Cdt1 fused to mCherry and truncated Geminin fused to mVenus. The two fusion proteins are always alternately expressed according to the cell cycle phase in the same ratio, making it possible to detect and quantify the number of labeled cells. By crossing rat insulin promoter (RIP)-Cre mice (mixed C57BL/6 and CBA/J background) (10) and R26Fucci2aR mice (mixed C57BL/6 and 129 background), we generated RIP-Cre; R26Fucci2aR mice expressing the Fucci2a reporter in a β -cell-specific manner. In these mice, mCherry-hCdt1 (red fluorescence) and mVenus-hGem (green fluorescence) are expressed in β -cell nuclei during the G₀/G₁ and S/G₂/M phase, respectively. The mice had free access to standard rodent chow and water and were housed in a temperature-controlled environment under a 14:10-h light/dark cycle. Animal care and protocols were reviewed and approved by the Kyoto University Graduate School of Medicine Animal Care and Use Committee (MedKyo15298), Kyoto, Japan.

Animal Experiments

S961 was obtained from Novo Nordisk (Bagsværd, Denmark). Vehicle (PBS) or 10 nmol S961 was loaded into an osmotic pump (Alzet 2001; DURECT Corp., Cupertino, CA) subcutaneously implanted into the back of RIP-Cre; R26Fucci2aR mice at 8 weeks of age. Mice were euthanized, and the pancreata were harvested 7 days after S961 or vehicle treatment. Blood glucose levels were measured daily. Plasma was collected on days 0 and 7 to measure insulin level. For a model of DIO, 6-week-old RIP-Cre; R26Fucci2aR mice were fed a high-fat diet (HFD; fat content, 60 kcal%) (cat. no. D12492; Research Diets) or a control diet (cat. no.

D12450J; Research Diets) for 13 weeks, and body weight was measured weekly. For pregnancy studies, 8-week-old RIP-Cre; R26Fucci2aR mice were interbred, and the pancreas was harvested at 14.5 days of gestation. A 50% PPTX was performed in 8-week-old RIP-Cre; R26Fucci2aR mice. The mice were anesthetized with isoflurane. The splenic portion of the pancreas was removed by gentle abrasion with cotton applicators and by partially breaking the mesenteric connections to the stomach, small bowel, and retroperitoneum. Mice in the sham group underwent laparotomy, and the pancreas was left intact. For the EdU-labeling assay, mice were intraperitoneally injected with EdU (50 mg/kg) 6 h before sacrifice. For the oral glucose tolerance test, mice were fasted for 16 h and then orally administered a 20% glucose solution (2 g/kg body weight). Blood samples were collected from the tail vein of mice 0, 15, and 30 min after glucose loading using heparinized calibrated glass capillary tubes (cat. no. 2-000-044-H; Drummond Scientific Co., Broomall, PA). Blood glucose level was measured using the Glutest Neo Sensor (Sanwa Kagaku Kenkyusho, Nagoya, Japan). Plasma samples were prepared by centrifuging the blood samples at 9,000g for 10 min, and the insulin level was measured using the Ultra Sensitive PLUS Mouse Insulin ELISA kit (cat. no. 49170-53; Morinaga, Tokyo, Japan).

Immunohistochemical Analysis of Pancreas

Mice were anesthetized by an intraperitoneal injection of pentobarbital sodium (10 mg/kg), a 26-gauge needle was inserted into the left ventricle through the apex, and the mice were transcardially perfused with ice-cold PBS, followed by ice-cold 4% paraformaldehyde (Wako Pure Chemical Industries, Osaka, Japan). The harvested pancreas was immediately immersed in paraformaldehyde 4°C with gentle shaking for <24 h and then embedded in optimal cutting temperature compound. Frozen samples were cut into 8- μ m sections. After air drying, the frozen sections were incubated with blocking buffer composed of PBS with 10% (v/v) goat serum and 0.2% (v/v) Triton-X100 for 30 min at room temperature. The sections were then incubated overnight at room temperature in blocking buffer supplemented with rabbit anti-insulin (200-fold dilution) (cat. no. ab181547), mouse anti-glucagon (2000-fold dilution) (cat. no. ab10988), rat anti-somatostatin (100-fold dilution) (cat. no. ab30788), or rabbit anti-Nkx 6.1 (100-fold dilution) (cat. no. ab221549) antibody (all from Abcam, Cambridge, MA), followed by Alexa Fluor 647-conjugated goat anti-rabbit IgG (H+L) (200-fold dilution) (cat. no. A-21245; Thermo Fisher Scientific, Waltham, MA), Alexa Fluor 647-conjugated goat anti-mouse IgG (H+L) (200-fold dilution) (cat. no. ab150115; Abcam), or Alexa Fluor 647-conjugated goat anti-rat IgG (H+L) (200-fold dilution) (cat. no. ab150159; Abcam) for 1 h at room temperature. The sections were incubated in PBS containing DAPI (final concentration: 0.01 mg/mL) for 15 min at room temperature and mounted with Vectashield (Vector Laboratories, Burlingame, CA) on 24- \times 40-mm coverslips (cat. no. C024401; Matsunami Glass, Osaka, Japan). Immunolabeled tissue sections were observed with

an inverted fluorescence microscope (BZ-X710; Keyence, Osaka, Japan). The Click-iT EdU Cell Proliferation Kit for Imaging (cat. no. C10340) and the Click-iT Plus TUNEL Assay for In Situ Apoptosis Detection (cat. no. C10619) were obtained from Thermo Fisher Scientific and used according to the manufacturer's protocol.

Tissue Clearing and 3D Imaging of Pancreas

Pancreas tissue samples were collected and fixed as described above and washed three times for more than 2 h each time in PBS at room temperature with gentle shaking. CUBIC reagents were obtained from Tokyo Chemical Industry Co., Ltd (cat. nos. T3740 and T3741). For delipidation and permeabilization, the samples were immersed in 50% (v/v) CUBIC-L clearing reagent for at least 6 h, followed by 100% (v/v) CUBIC-L at 37°C with gentle shaking for 3 days. The CUBIC-L reagent was refreshed daily during this period. After clearing, samples were immersed in 50% (v/v) CUBIC-R for at least 6 h and in 100% (v/v) CUBIC-R at room temperature with gentle shaking for at least 2 days. 3D images of optically cleared pancreas tissue were acquired with a light-sheet microscope (Lightsheet Z.1; Carl Zeiss, Oberkochen, Germany) equipped with a 5 \times /0.16 numerical aperture objective lens. For mCherry-hCdt1 imaging, 22% laser power (561-nm laser) and a 28-ms exposure time were used. For mVenus-hGem imaging, 90% laser power (488-nm laser) and a 70-ms exposure time were used. The z-stack images (1,920 \times 1,920 pixel, 16-bit) were acquired at 4.63- μ m intervals.

Image Processing

Acquired images were analyzed with the 3D reconstruction software Imaris (Bitplane AG, Zurich, Switzerland). A whole series of consecutive two-dimensional cross-sectional images was reconstructed into a 3D structure using the "Volume rendering" function. Each islet was then isolated using the "Crop 3D function," and a Gaussian filter was applied for background noise reduction. The Imaris "Spot" algorithm was used to identify β -cells from mCherry or mVenus signals with "Background subtraction." The estimated detection diameter was set to 10 μ m, and the "Quality" filter with the threshold value adjusted automatically (for mCherry) and manually (for mVenus) was applied. The diameter of the β -cell clusters (i.e., mCherry-signal cluster) was calculated by the Imaris "Surface" function, rendering the mCherry-signal clusters into 3D objects and measuring their maximum diameter automatically.

Intravital Imaging

After S961 treatment for 40 h, RIP-Cre; Fucci2aR mice were anesthetized by 1.5–2% isoflurane (Wako Pure Chemical Industries) inhalation. The hair on the abdominal area was removed and the skin disinfected with 70% ethanol. A small oblique incision running parallel to the last left rib was made to expose the pancreas on the left side of the abdominal wall. The mice were then placed supine on an electric heating pad maintained at 37°C. The pancreas was

immobilized using a suction imaging device (Supplementary Fig. 2), and time-lapse imaging was performed with a two-photon excitation microscope (FV1200MPE-BX61WI; Olympus, Tokyo, Japan) equipped with a 25 \times /1.05 numerical aperture water-immersion objective lens (XLPLN 25XWMP; Olympus) and an In-Sight DeepSee Ultrafast laser (Spectra Physics, Santa Clara, CA). Images were acquired every 5 min for \sim 10 h in 5- μ m steps at a scan speed of 20 μ s/pixel. Mice were euthanized after imaging.

Quantification and Statistical Analysis

The Mann-Whitney *U* test was performed to evaluate the difference between two sets of data. *P* values $<$ 0.05 were considered statistically significant. No statistical method was used to predetermine sample size. Statistical analyses were performed using GraphPad Prism (GraphPad Software, La Jolla, CA).

Data and Resource Availability

The data sets generated during the current study are available from the corresponding author upon reasonable request. No applicable resources were generated or analyzed during the current study.

RESULTS

Generation and Characterization of RIP-Cre; R26Fucci2aR Mice

To distinguish β -cells in the G_0/G_1 phase from those in $S/G_2/M$ phase, we used Fucci technology, which is a proven tool for detecting actively proliferating cells (3). The R26Fucci2aR mouse line harboring the Fucci2a reporter was recently generated, in which Cre/loxP-mediated conditional expression of the Fucci2a transgene at the Rosa26 locus is driven by the cytomegalovirus early enhancer/chicken β -actin promoter (9). By crossing rat RIP-Cre and R26Fucci2aR mice, we generated the RIP-Cre; R26Fucci2aR line, in which the Fucci2a probe is specifically expressed in β -cells (Fig. 1A). RIP-Cre; R26Fucci2aR mice showed similar body weight and random-fed blood glucose levels compared with R26Fucci2aR littermates (Fig. 1B and C), and there was no significant difference in blood glucose and insulin levels during the oral glucose tolerance test (2 g/kg) between them (Fig. 1D and E), indicating that RIP-Cre; R26Fucci2aR mice have normal glucose tolerance and insulin secretion.

We then investigated the expression pattern of the Fucci2a probe in RIP-Cre; R26Fucci2aR mice. To characterize not only mCherry⁺ but also mVenus⁺ cells, we induced β -cell proliferation in RIP-Cre; R26Fucci2aR mice by continuous infusion of the vehicle PBS or insulin receptor antagonist S961 for 7 days using an osmotic pump. At the end of the treatment, frozen sections were prepared from the dissected pancreas and immunostained for insulin, glucagon, somatostatin, and Nkx-6.1, and the fluorescent signals of the Fucci2a probe were directly observed. In both vehicle and S961-treated RIP-Cre; R26Fucci2aR mice, mCherry and mVenus were expressed specifically in insulin⁺ and Nkx 6.1⁺ cells (Fig. 2A and B and Supplementary Fig. 1A and B),

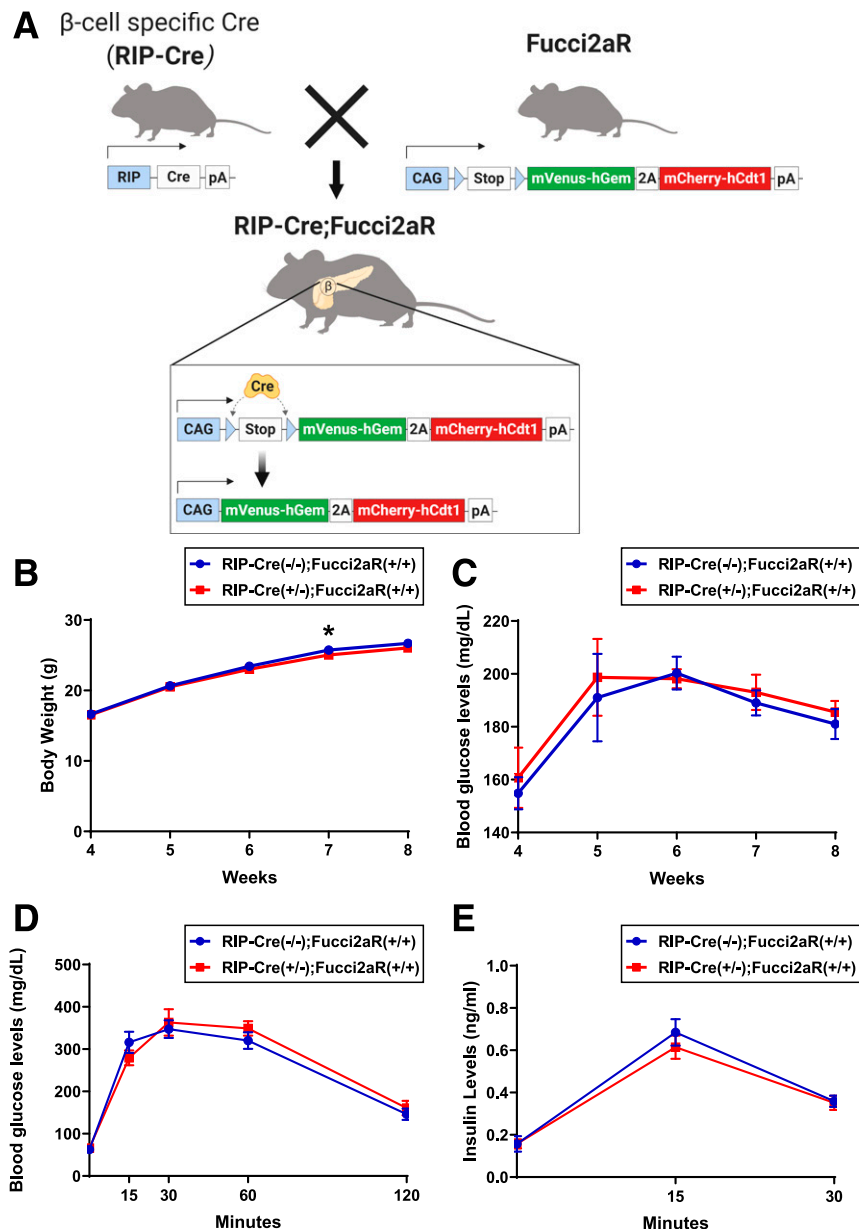


Figure 1—Genotype and metabolic phenotype of RIP-Cre; Fucci2aR mice. **A**: Breeding scheme for the generation of RIP-Cre; Fucci2aR mice. RIP-Cre and Fucci2aR mouse lines were crossed to obtain RIP-Cre; Fucci2aR mice. After Cre-mediated recombination, the Fucci2a transgene was expressed specifically in β -cells. Body weight (**B**) and random-fed blood glucose levels of RIP-Cre^(+/-); Fucci2aR^(+/+) ($n = 7$) and control littermates (RIP-Cre^(-/-); Fucci2aR^(+/+)) ($n = 7$) mice during postnatal growth (**C**). **D** and **E**: Oral glucose tolerance test (2 g/kg body wt) performed on RIP-Cre; Fucci2aR ($n = 7$) and control littermates ($n = 7$) mice at 8 weeks. Data are expressed as mean \pm SEM. * $P < 0.05$ (Mann-Whitney U test).

but not in glucagon⁺ or somatostatin⁺ cells (Fig. 2C and D and Supplementary Fig. 1C and D). To ensure that replicating β -cells could be quantified, we compared the results of the EdU assay and the β -cell proliferation assay performed using RIP-Cre; R26Fucci2aR mice treated by S961. The fluorescence images demonstrated that only mCherry⁻ mVenus⁺ cells were labeled by EdU, but not mCherry⁺ mVenus⁺ cells (Fig. 2E and Supplementary Fig. 1E). MetaMorph software (Molecular Devices) was used to count mVenus⁺ cells (Fig. 3A) or EdU⁺ insulin⁺ DAPI⁺ cells (Fig.

3B) in frozen sections. We confirmed that the numbers of EdU⁺ insulin⁺ cells per insulin⁺ cells and the numbers of mVenus⁺ cells per mCherry⁺ mVenus⁻ cells + mCherry⁻ mVenus⁺ cells in the S961-treated group were similarly higher than those in control group. We also evaluated β -cell proliferation in RIP-Cre; R26Fucci2aR mice in response to DIO and confirmed that the numbers of EdU⁺ insulin⁺ cells per insulin⁺ cells and the numbers of mVenus⁺ cells per mCherry⁺ mVenus⁻ cells + mCherry⁻ mVenus⁺ cells in DIO group were similarly higher than those in control group (Fig. 3C and D).

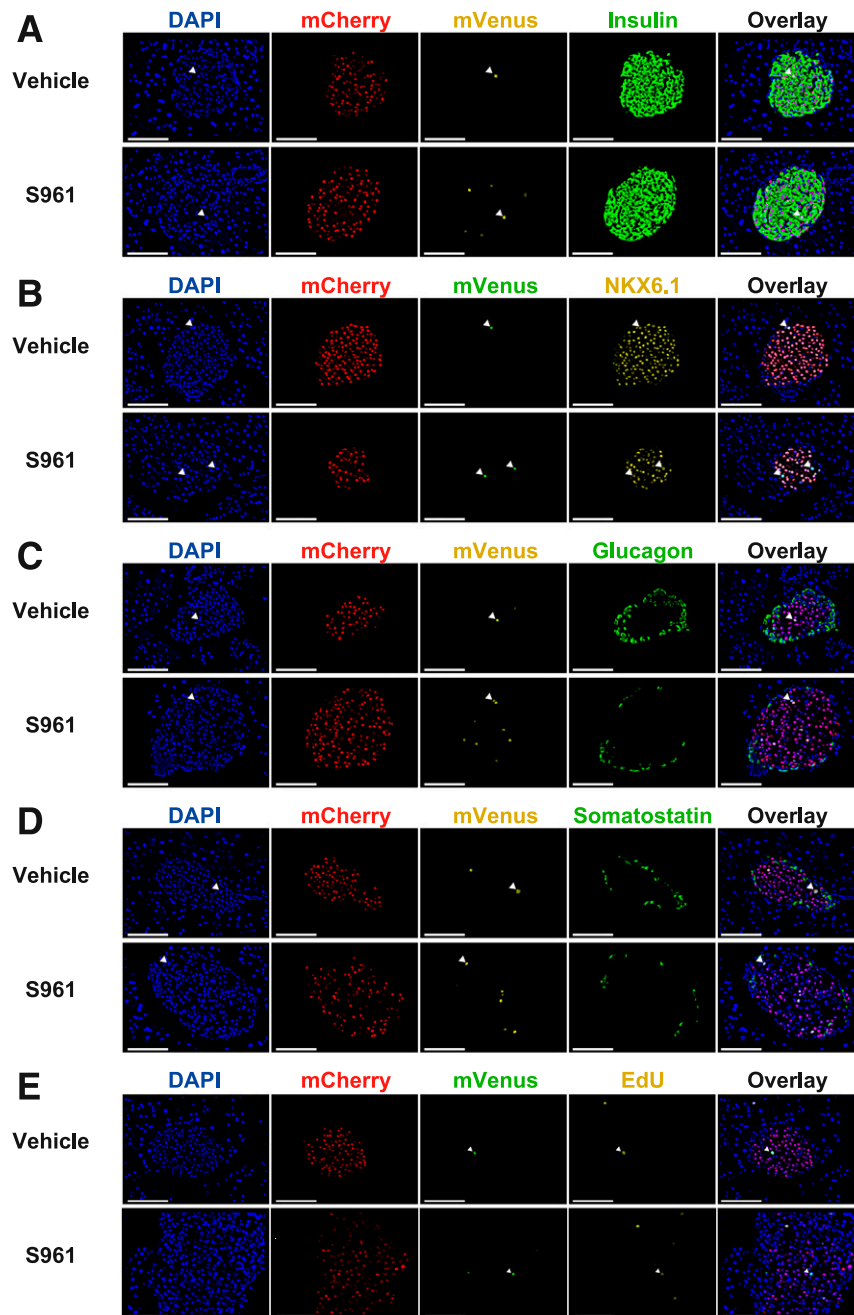


Figure 2— β -Cell-specific expression of Fucci2a in RIP-Cre; R26Fucci2aR mice. *A–E*: Frozen sections of pancreas tissues from RIP-Cre; R26Fucci2aR mice treated with S961 or vehicle at 8 weeks of age immunostained for islet hormones, Nkx 6.1, and EdU (original magnification $\times 40$). Representative fluorescence images of mCherry⁺ (red) and mVenus⁺ (yellow, arrowheads) cells and immunofluorescence for islet hormones (green): insulin (*A*), glucagon (*C*), and somatostatin (*D*). While 269–280 islets from eight pancreata (four vehicle-treated mice and four S961-treated mice) were analyzed, no glucagon⁺ areas and somatostatin⁺ areas were merged with mCherry⁺ and/or mVenus⁺ cells. *B*: All mCherry⁺ (red) and mVenus⁺ (green, arrowheads) cells were Nkx 6.1⁺ (yellow). Nuclei were stained with DAPI (blue). *E*: Frozen sections were labeled by EdU. Note that only mCherry[–] mVenus⁺ cells (green, arrowhead) were labeled by EdU (yellow). Scale bars, 100 μ m.

3D Imaging of Islets in RIP-Cre; R26Fucci2aR Mice

Because each islet is densely packed with various cell types, replicating β -cells can be misidentified in histological sections labeled for insulin and replication markers. In order to detect and quantify replicating β -cells in 3D in whole islets of RIP-Cre; R26Fucci2aR mice, CUBIC clearing

reagent (11) was applied to pancreatic tissue samples from vehicle- or S961-treated RIP-Cre; R26Fucci2aR mice, and 3D images of the optically cleared tissue were obtained with a light-sheet microscope equipped with a $5\times$ objective lens. The spatial distributions of mVenus⁺ and mCherry⁺ cells were simultaneously visualized (Fig. 4A–F and

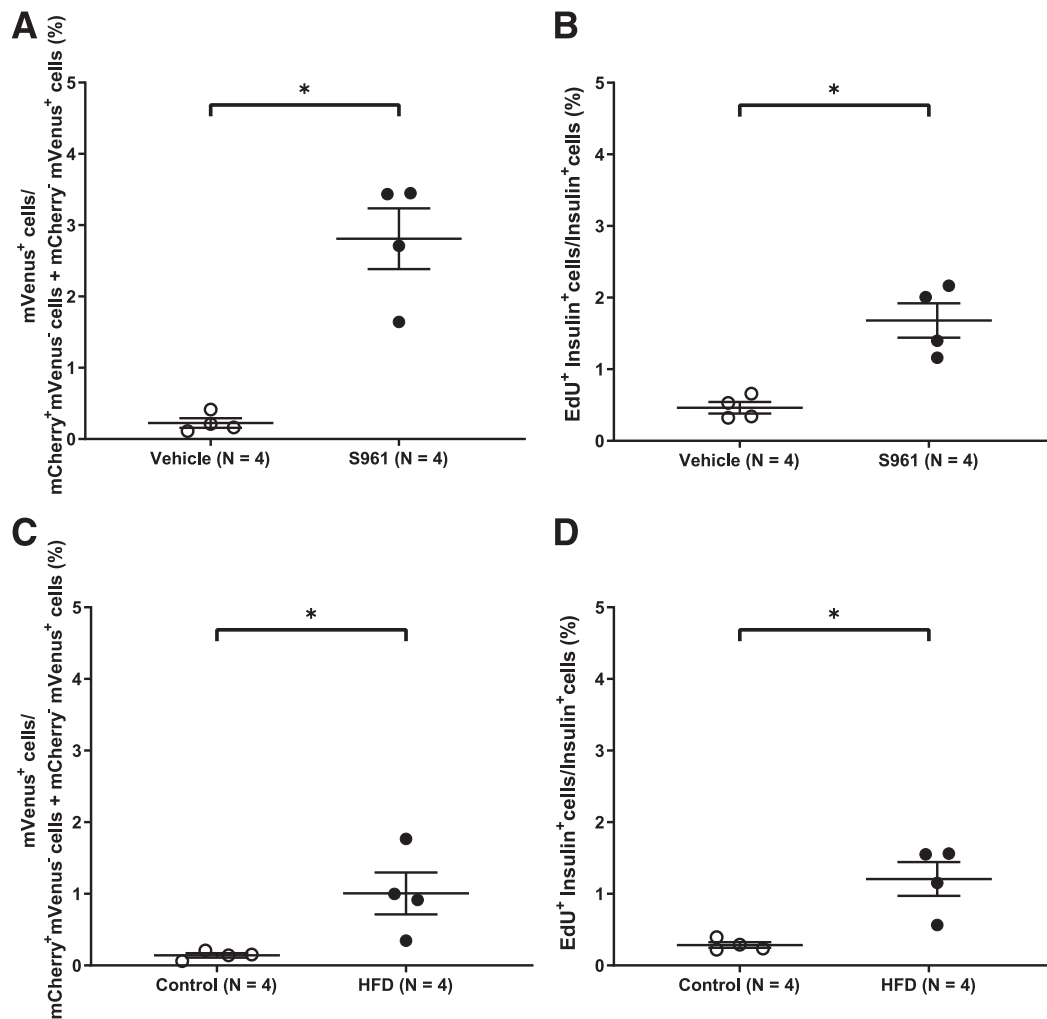


Figure 3—Comparison of replicating β -cell quantification by Fucci2a probes with EdU assay. *A*: Quantification of mVenus⁺ cells in the islets of RIP-Cre; R26Fucci2aR mice treated with PBS (vehicle; $n = 4$) or S961 (10 nmol/week; $n = 4$). *B*: Quantification of EdU⁺ insulin⁺ cells in islets of RIP-Cre; R26Fucci2aR mice treated with PBS (vehicle; $n = 4$) or S961 (10 nmol/week; $n = 4$). *C*: Quantification of mVenus⁺ cells in the islets of RIP-Cre; R26Fucci2aR mice fed the control diet ($n = 4$) or HFD ($n = 4$). *D*: Quantification of EdU⁺ insulin⁺ cells in islets of RIP-Cre; R26Fucci2aR mice fed the control diet ($n = 4$) or HFD ($n = 4$). In vehicle- and S961-treated group, 1,386–8,368 insulin⁺ cells and 1,291–2,837 mCherry⁺ mVenus⁻ cells + mCherry⁻ mVenus⁺ cells were counted per mouse. In the control and HFD groups, 2,411–6,976 insulin⁺ cells and 1,922–4,919 mCherry⁺ mVenus⁻ cells + mCherry⁻ mVenus⁺ cells were counted per mouse. Data are expressed as mean \pm SEM. * $P < 0.05$.

Supplementary Video 1). Islets contained more mVenus⁺ cells after S961 treatment (Fig. 4C and D). Spot objects corresponding to mVenus⁺ or mCherry⁺ cells were reconstructed using Imaris Spot Detection and quantified by an automated process to determine the number of replicating β -cells in each islet (Fig. 4G and H). The Imaris Surface tool was used to measure the diameter of β -cell clusters in each islet. Thus, RIP-Cre; R26Fucci2aR mice are amenable to cross-sectional analyses of the number and spatial distribution of proliferating β -cells.

Given the utility of the Fucci2a probe for real-time monitoring of the cell cycle, we performed real-time in vivo imaging in S961-treated RIP-Cre; R26Fucci2aR mice using a two-photon microscope equipped with a 25 \times water objective lens. This intravital imaging of an islet in

a RIP-Cre; R26Fucci2aR mouse initiated 40 h after S961 treatment revealed the S-phase progression of β -cells (Supplementary Fig. 2 and Supplementary Video 2). We also detected one mCherry⁺ mVenus⁺ cell for >8 h (Supplementary Video 3).

The Number of Replicating β -Cells per Islet Is Positively Correlated With Islet Size

The relationship between the number of replicating β -cells per islet and the morphological characteristics of the islets is unclear. We addressed this issue by analyzing 3D images obtained from RIP-Cre; R26Fucci2aR mice using the 3D reconstruction software Imaris. Blood glucose and insulin levels were higher in mice treated with S961 than in those treated with vehicle (Fig. 5A and B). When we examined all

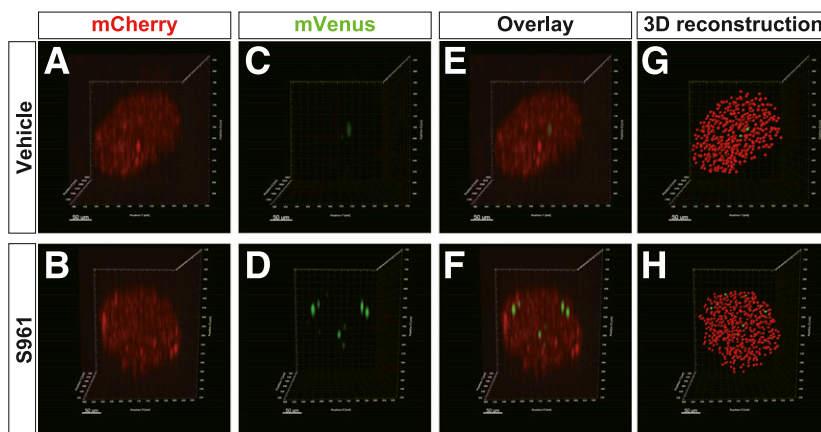


Figure 4—Representative 3D imaging of islets in vehicle- and S961-treated RIP-Cre; R26Fucci2aR mice after treatment for 1 week. Representative fluorescence images of mCherry⁺ (red) (A and B) and mVenus⁺ (green) cells (C and D), and overlay (E and F). G and H: Morphological 3D reconstruction of mCherry⁺ (red) and mVenus⁺ (green) cells for automated cell counting. Images were obtained with a light-sheet microscope. Scale bars, 50 μ m.

islets with β -cell cluster diameter $>100 \mu\text{m}$, the β -cell cluster diameter (i.e., mCherry-signal cluster diameter) and β -cell number per islet (i.e., the number of mCherry signals and mVenus signals per islet) were greater in S961-treated RIP-Cre; R26Fucci2aR mice (Fig. 5C–E). In addition, the proportion of mVenus⁺ cells per islet was higher in S961-treated mice compared with that in control mice (Fig. 5F). Moreover, the mVenus⁺ cell number per islet was positively correlated with the β -cell number per islet in both vehicle-treated (Fig. 5G) ($r = 0.77$, $P < 0.0001$) and S961-treated (Fig. 5G) ($r = 0.87$, $P < 0.0001$) mice. As an exploratory research, we also tested whether S961-induced β -cell proliferation is due to hyperglycemia using a sodium–glucose cotransporter 2 inhibitor that enhances urinary glucose excretion and normalizes hyperglycemia-associated S961 administration. While it has been shown that hyperglycemia induces β -cell proliferation (12,13), near-normalization of hyperglycemia associated with S961 administration by sodium–glucose cotransporter 2 inhibitor treatment increased the β -cell number per islet (Supplementary Fig. 3). These results suggest that hyperglycemia itself has limited effects on S961-induced β -cell proliferation.

We then investigated whether this positive correlation also exists under other physiological conditions such as DIO, pregnancy, and PPTX. The RIP-Cre; R26Fucci2aR mice were divided into two groups: one fed the HFD and the other fed the control diet for 13 weeks. The HFD group gained significantly more body weight than control diet group during the 13-week period (Fig. 6A). Compared with the control diet group, the HFD group showed larger β -cell cluster diameter (Fig. 6B and C), β -cell number per islet (Fig. 6D), and proportion of mVenus⁺ cells per islet (Fig. 6E). Although the pregnant group showed no significant difference in β -cell number per islet (Fig. 7C) compared with the virgin group, its β -cell cluster diameter (Fig. 7A and B) was larger, and its proportion of mVenus⁺ cells per islet (Fig. 7D) was higher. Finally, the

positive correlation between the mVenus⁺ cell number per islet and the β -cell number per islet was also found in the HFD group (Fig. 6F) ($r = 0.81$, $P < 0.0001$) and in the pregnant group (Fig. 7E) ($r = 0.90$, $P < 0.0001$). Regarding PPTX, although β -cell cluster diameter in the PPTX group was as large as that in sham group 2 days after the operation (Fig. 8A and B), the PPTX group showed fewer β -cell numbers per islet (Fig. 8C). However, the number of mVenus⁺ cells per islet was significantly higher (Fig. 8D) and was positively correlated with the β -cell number per islet in the PPTX group (Fig. 8E) ($r = 0.49$, $P < 0.0001$). These data indicate that islets with a larger population of β -cells have more replicating β -cells.

DISCUSSION

In the current study, we generated and characterized a novel mouse line (i.e., RIP-Cre; R26Fucci2aR mice) that enables a quantitative analysis of replicating β -cells in a spatiotemporal manner. β -Cell proliferation analysis has been traditionally performed by immunohistochemical assay using BrdU or EdU labeling. However, these results are occasionally inaccurate and unreproducible due to the inherent limitations. A recent study reported interlaboratory variability in the immunohistochemical detection of Ki-67 for identification of β -cells as well as quantification of their replication; the authors concluded that the discrepancy among laboratories was due to the misidentification of replicating non- β -cells within islets as β -cells (2). Because several different cell types are densely packed in the sphere-like islets, analysis of two-dimensional immunohistochemical data might well lead to inaccuracies in detection of β -cells. Moreover, the nucleotide analog BrdU, which is often used as a cell cycle marker in traditional immunohistochemical assays, has unfavorable effects on the cell cycle of β -cells (14), especially in causing underestimation the β -cell proliferation rate. The aim of our

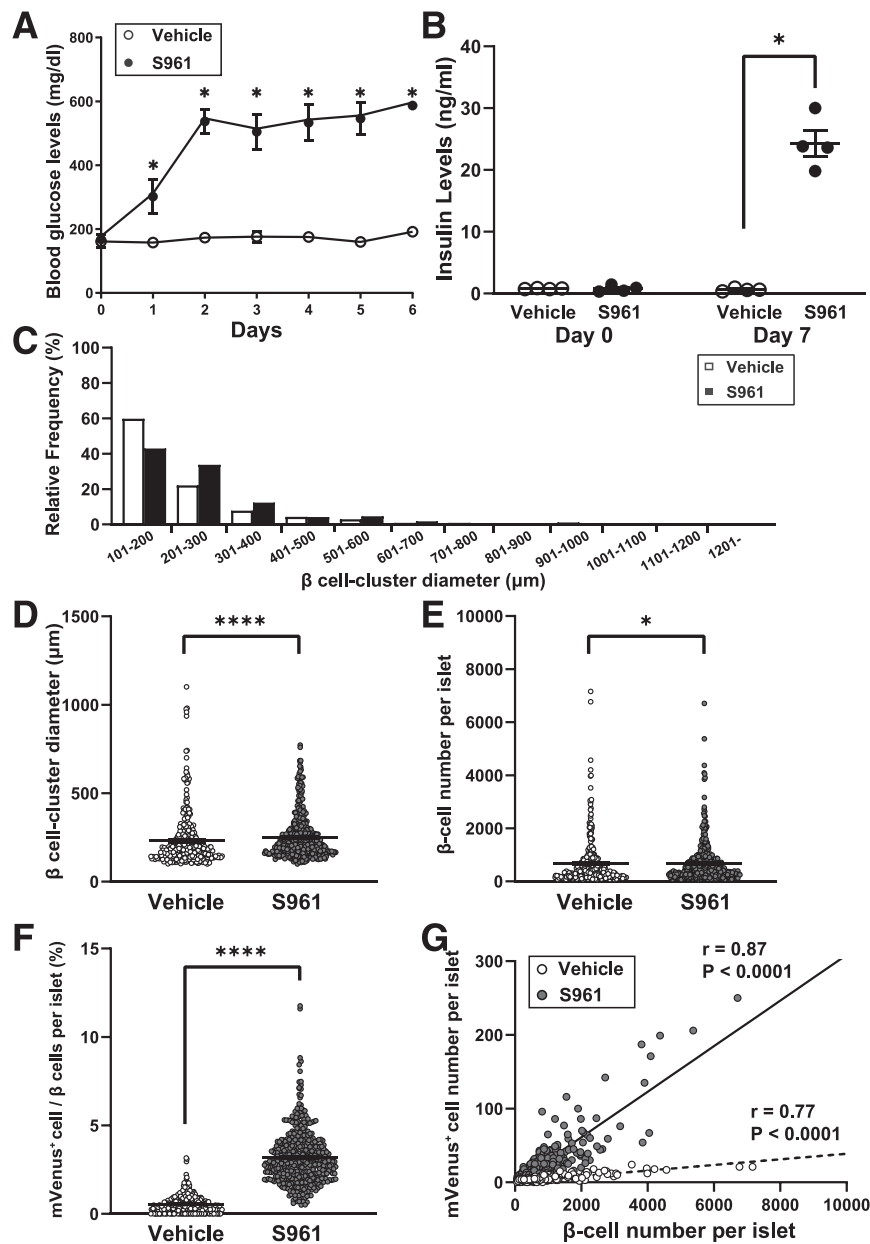


Figure 5—Quantification of replicating β -cells in RIP-Cre; R26Fucci2aR mice after S961 treatment. *A* and *B*: RIP-Cre; R26Fucci2aR mice were treated with S961 (10 nmol/week) ($n = 4$) or PBS (vehicle; $n = 4$) for 7 days. Random-fed blood glucose (*A*) and serum insulin (*B*) levels at the end of the 7-day PBS and S961 treatment. *C*–*G*: Morphometric analysis was performed on islets harboring β -cell clusters with diameter $>100 \mu\text{m}$ (S961, 454 islets from four mice; and vehicle, 348 islets from four mice). *C*: Histogram of β -cell cluster diameter. *D*: β -Cell cluster diameter. *E*: Number of β -cells per islet. *F*: Percentage of mVenus⁺ cells per islet. *G*: Correlation between number of mVenus⁺ cells and number of β -cells per islet. mVenus⁺ cell number and β -cell number per islet was strongly correlated in both groups (S961, $r = 0.87$, $P < 0.0001$; vehicle, $r = 0.77$, $P < 0.0001$). Data are presented as mean \pm SEM. * $P < 0.05$ and **** $P < 0.0001$.

study is to establish an alternative method that overcomes these weaknesses.

Fucci2a, a single fluorescence probe for monitoring cell cycle transition, differentiates cells in G_0/G_1 from those in the $S/G_2/M$ phase based on mCherry-hCdt1 and mVenus-hGem expression (3). By establishing RIP-Cre; R26Fucci2aR mice in which Fucci2a is expressed specifically in β -cells, we have established an alternative and more accurate assay for proliferating β -cells. In high magnification images

(Supplementary Fig. 1A), we observed several mCherry[−] mVenus[−] insulin⁺ cells which could be either β -cells without Fucci probe expression or β -cells immediately after mitosis. If mCherry[−] mVenus[−] insulin⁺ cells are composed mainly of the latter, their proportion among total β -cells should be higher in the S961-treated group. However, no significant difference in their proportion was found between the vehicle- and S961-treated groups (data not shown). This might suggest that such mCherry[−] mVenus[−] insulin⁺ cells

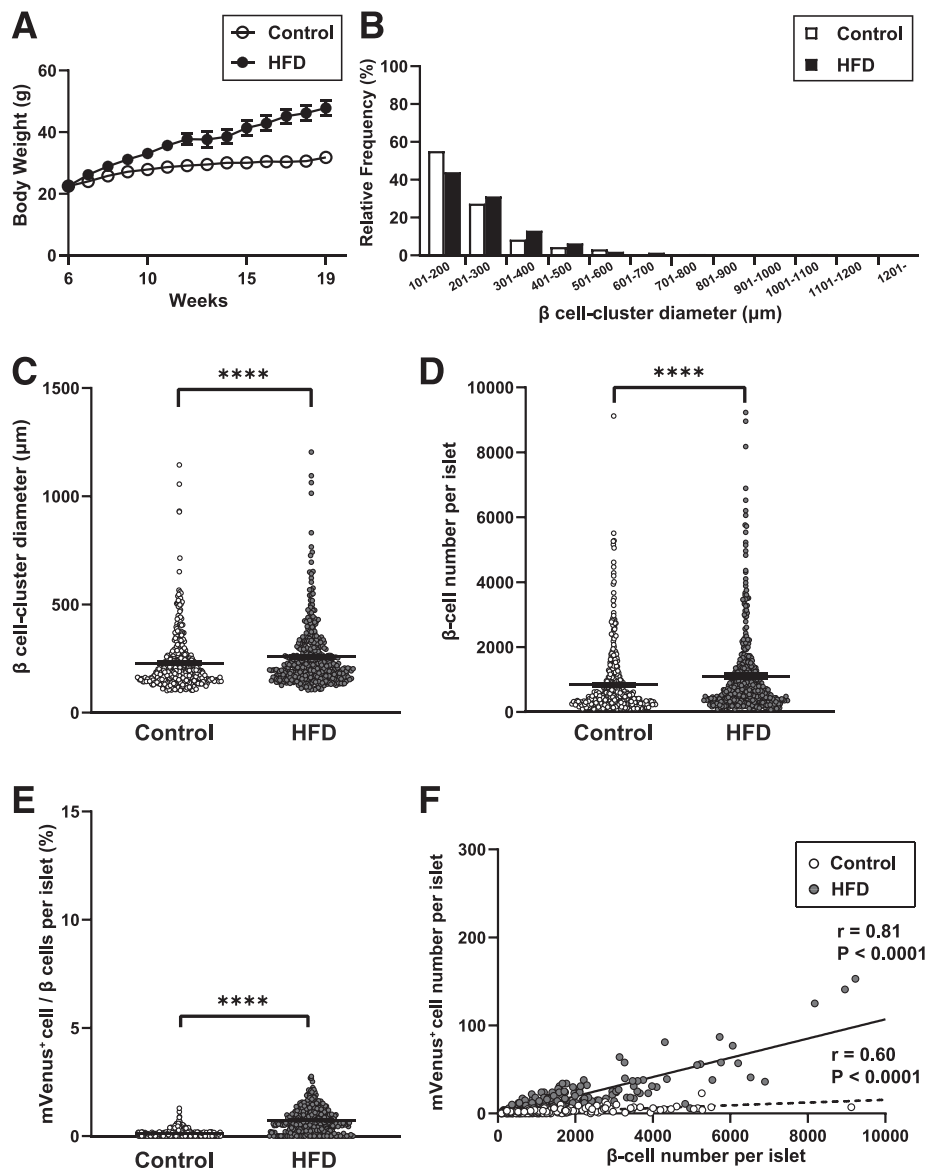


Figure 6—Quantification of replicating β -cells in RIP-Cre; R26Fucci2aR mice fed the control diet or the HFD. **A**: Body weight of RIP-Cre; R26Fucci2aR mice fed the HFD ($n = 7$) or control diet ($n = 7$) for 13 weeks. **B–F**: Morphometric analysis was performed on islets harboring β -cell clusters with diameter $>100 \mu\text{m}$ (HFD, 407 islets from four mice; control, 432 islets from four mice). **B**: Histogram of β -cell cluster diameter. **C**: β -Cell cluster diameter. **D**: Number of β -cells per islet. **E**: Percentage of mVenus⁺ cells per islet. **F**: Correlation between number of mVenus⁺ cells and number of β -cells per islet. mVenus⁺ cell number and β -cell number per islet were strongly correlated in both groups (HFD, $r = 0.81$, $P < 0.0001$; control diet, $r = 0.60$, $P < 0.0001$). Data are presented as mean \pm SEM. **** $P < 0.0001$.

were rarely detected because mCherry[−] mVenus[−] duration was the shortest among other phases of the cell cycle (3).

In frozen sections, we also found that many mVenus⁺ cells were mCherry⁺. Because these cells were not labeled by EdU (Fig. 2E and Supplementary Fig. 1E), they might be β -cells during G₁-S transition. These mCherry⁺ mVenus⁺ cells could suggest prolonged G₁-S transition or an unknown cell cycle restriction in response to S961. This is also supported by the finding that one β -cell remained mCherry⁺ mVenus⁺ for >8 h according to the intravital imaging data (Supplementary Video 3). While the number of replicating β -cells that can be analyzed in our intravital

imaging is presently limited and it is difficult to draw definitive conclusions, these findings suggest the utility of our tool to investigate cell cycle regulation and kinetics of β -cells in the future.

Since RIP-Cre; R26Fucci2aR mice label a proliferative β -cell pool, 3D analysis of optically cleared pancreas of these mice enables measurement of the β -cell proliferation rate unaffected by replicating non- β -cells. In addition, 3D analysis allows sampling of β -cells from whole islets, which increases the sample size and provides spatial information on the replicating β -cells within an islet. As a result, the correlation between the β -cell proliferative capacity and

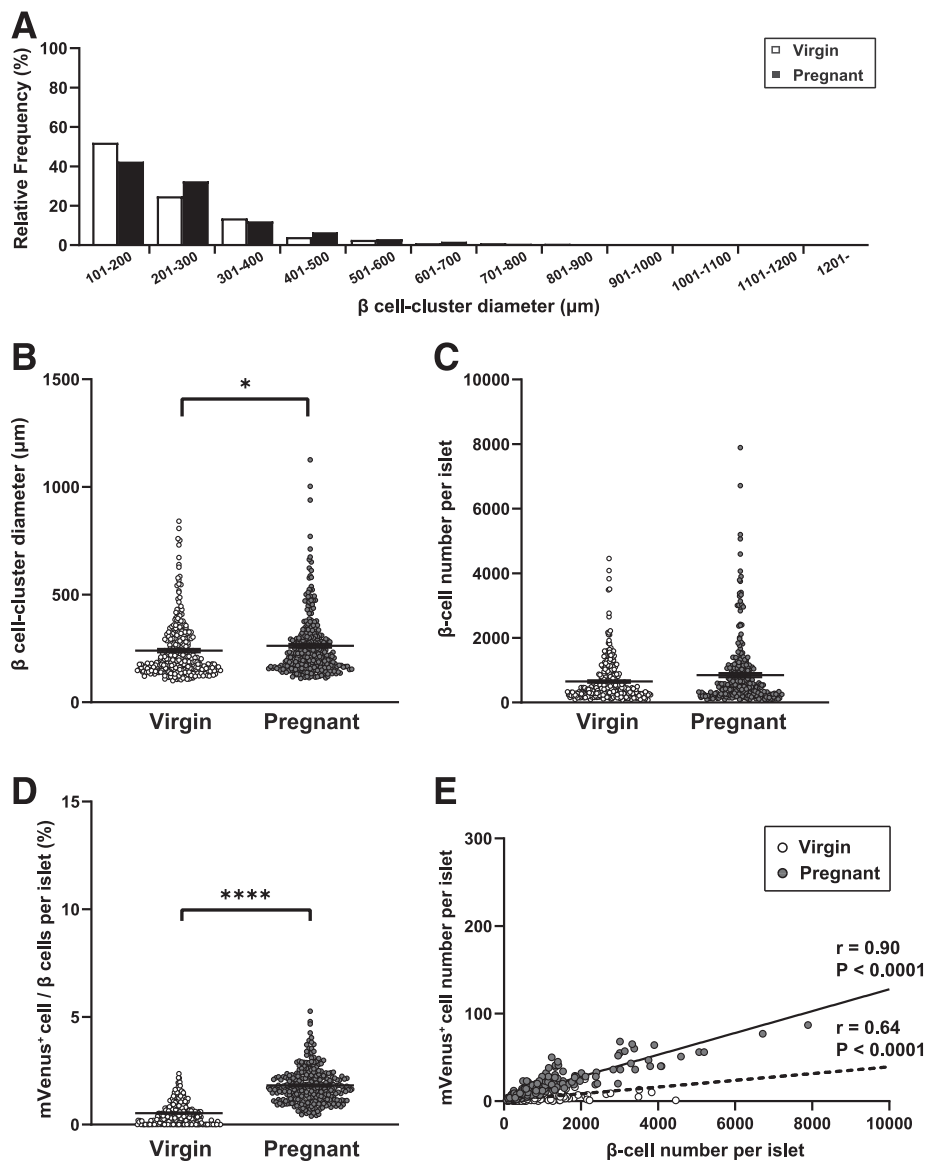


Figure 7—Quantification of replicating β -cells in pregnant (gestational days 14.5 of pregnancy) or virgin RIP-Cre; R26Fucci2aR mice. *A–E*: Morphometric analysis was performed on islets harboring β -cell clusters with diameter $>100\ \mu\text{m}$ (pregnant, 290 islets from four mice; virgin, 294 islets from four mice). *A*: Histogram of β -cell cluster diameter. *B*: β -Cell cluster diameter. *C*: Number of β -cells per islet. *D*: Percentage of mVenus⁺ cells per islet. *E*: Correlation between number of mVenus⁺ cells and number of β -cells per islet. mVenus⁺ cell number and β -cell number per islet were strongly correlated in both groups (pregnant, $r = 0.90$, $P < 0.0001$; virgin, $r = 0.64$, $P < 0.0001$). Data are presented as mean \pm SEM. * $P < 0.05$ and **** $P < 0.0001$.

the morphological characteristics of each islet can be established. Although some improvements to our system are required to keep the animals alive long enough to monitor the entire time course of β -cell proliferation, our intravital imaging data demonstrates that longitudinal spatiotemporal data on β -cell proliferation can be obtained from RIP-Cre; R26Fucci2aR mice (Supplementary Videos 2 and 3).

The 3D analysis of the pancreas of RIP-Cre; R26Fucci2aR mice revealed differing rates of β -cell proliferation within each islet under various interventions such as S961 treatment, DIO, pregnancy, and PPTX. By comparing these four models, we found that in our experimental conditions, S961

treatment induces the highest β -cell proliferation rate, followed by pregnancy, PPTX, and DIO (Supplementary Fig. 4). When we counted all mCherry⁺ and mVenus⁺ cells as β -cells, we found that the total number of β -cells per islet was increased by S961 treatment and DIO. This is consistent with previous reports on S961 and DIO-induced β -cell proliferation and mass expansion (4,5). However, we found the difference in β -cell cluster diameter and the number of β -cells per islet between the vehicle and S961 groups was surprisingly small. Our TUNEL assay found that S961 treatment caused significantly more β -cell apoptosis (Supplementary Fig. 5). The intravital imaging also

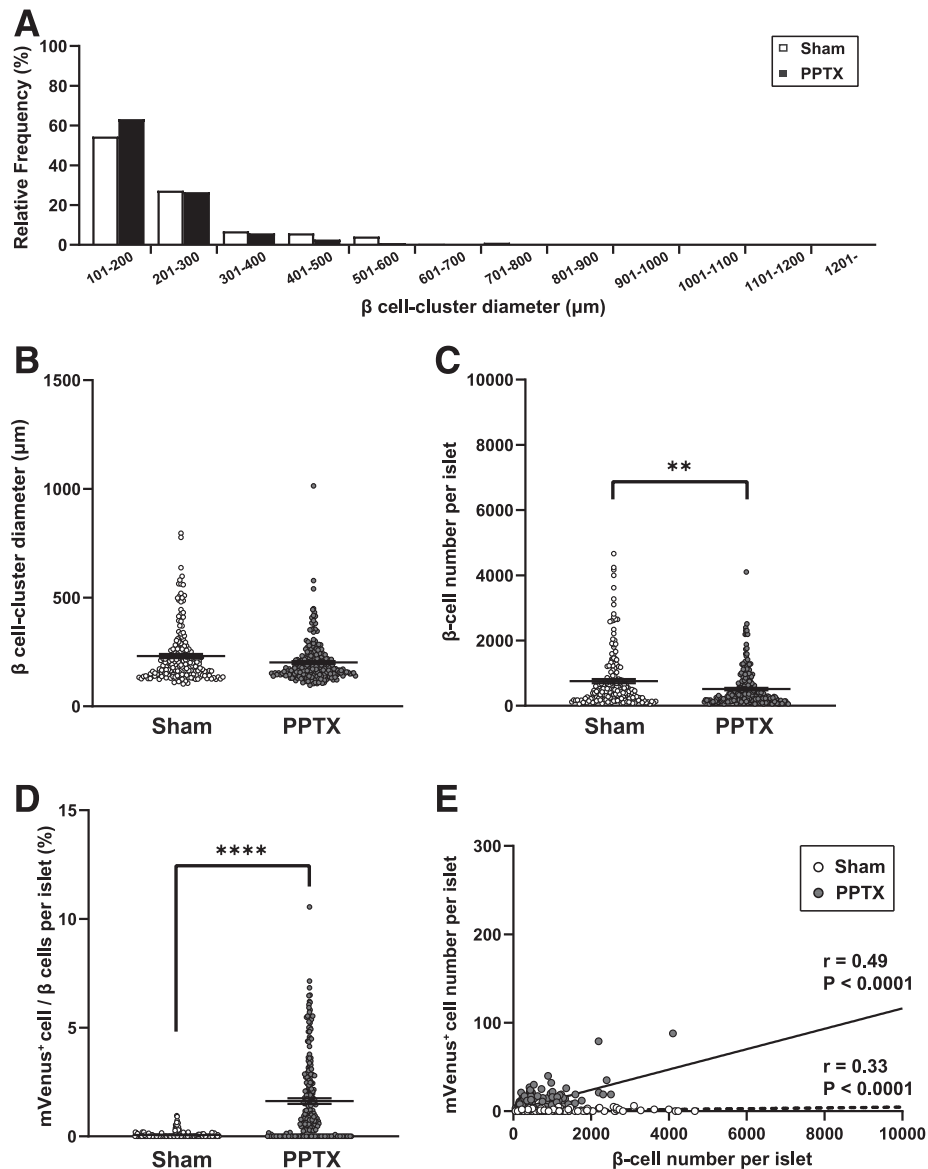


Figure 8—Quantification of replicating β -cells in RIP-Cre; R26Fucci2aR mice 2 days after 50% PPTX or sham operation. A–E: Morphometric analysis was performed on islets harboring β -cell clusters with diameter $>100\ \mu\text{m}$ (PPTX, 226 islets from four mice; sham, 191 islets from four mice). A: Histogram of β -cell cluster diameter. B: β -Cell cluster diameter. C: Number of β -cells per islet. D: Percentage of mVenus⁺ cells per islet. E: Correlation between number of mVenus⁺ cells and number of β -cells per islet. mVenus⁺ cell number and β -cell number per islet were strongly correlated in both groups (PPTX, $r = 0.49$, $P < 0.0001$; sham, $r = 0.33$, $P < 0.0001$). Data are presented as mean \pm SEM. ** $P < 0.01$ and **** $P < 0.0001$.

captured mVenus⁺ cells undergoing apoptosis in S961-treated mice (Supplementary Video 3). Considering these findings together, the small difference may be due to apoptosis of β -cells including mVenus⁺ cells caused by profound hyperglycemia concomitant with S961 treatment. On the other hand, there was no significant difference in the total number of β -cells per islet between the pregnant and virgin groups. This is possibly because the pancreata were harvested at ~ 14.5 days of gestation when β -cell proliferation reaches its peak, while β -cell mass does so at later stages during pregnancy (15). The similar scenario could be applicable to our PPTX experiments. Samples were analyzed

2 days after the operation, which might be too soon to detect an increase in the total number of β -cells per islet. In addition, the strong positive correlation between mVenus⁺ cells and the total β -cell number per islet suggests that islets comprising a greater number of β -cells contain more replicating β -cells.

Our study has several limitations. First, because only β -cells were labeled by the Fucci2a probe, other endocrine cells within islets could not be detected in RIP-Cre; R26Fucci2aR mice. Therefore, mitogenic effects on non- β -cells must be investigated using other methods. Second, the attenuation of fluorescence by light scattering limited the observation

depth from the pancreas surface. Such signal attenuation is unavoidable despite the optical clearing process. Under the light-sheet microscope, only islets near (~2.0 mm from) the surface were clearly detected for quantification of fluorescent cells. Although this restricts the size of islet population, the sample size is still larger using our method compared with a conventional immunohistochemical assay because it is based on 3D analysis of whole pancreas.

In summary, the current mouse line expressing the Fucci2a probe in β -cells serves as a new tool that allows spatiotemporal analysis in a quantitative manner of β -cell proliferation in response to mitogen stimulation.

Acknowledgments. The authors thank Asako Sakaue-Sawano and Atsushi Miyawaki (RIKEN Center for Brain Science, Wako, Saitama, Japan) and Tomonobu Hatoko (Department of Diabetes, Endocrinology and Nutrition, Kyoto University) for their scientific discussion; Saki Kanda and Sara Yasui (Department of Diabetes, Endocrinology and Nutrition, Kyoto University) for technical assistance; and Yukiko Inokuchi, Yukiko Tanaka, and Fumiko Uwamori (Department of Diabetes, Endocrinology and Nutrition, Kyoto University) for secretarial assistance.

Funding. This work was supported by grants from Japan Society for the Promotion of Sciences (KAKENHI grant numbers 26111004, 17K09825, and 17K19654). This work was also supported by the Kyoto University Live Imaging Center and in part by Grants-in-Aid KAKENHI 16H06280 “ABIS.”

Duality of Interest. D.Y. received consulting or speaking fees from MSD K.K., Nippon Boehringer Ingelheim Co. Ltd., and Novo Nordisk Pharma Ltd., and received clinically commissioned/joint research grants from Taisho Toyama Pharmaceutical Co. Ltd., MSD K.K., Ono Pharmaceutical Co. Ltd., Novo Nordisk Pharma Ltd., Arklay Co. Ltd., Terumo Co. Ltd., and Takeda Pharmaceutical Co. Ltd. N.I. received clinical commissioned/joint research grants from Mitsubishi Tanabe, AstraZeneca, Astellas, and Novartis Pharma, and scholarship grants from Takeda, MSD, Ono, Sanofi, Japan Tobacco Inc., Mitsubishi Tanabe, Novartis, Boehringer Ingelheim, Kyowa Kirin, Astellas, and Daiichi-Sankyo. No other potential conflicts of interest relevant to this article were reported.

Author Contributions. S.T. analyzed the data. S.T., D.Y., and N.I. designed the study. S.T., D.Y., and N.I. wrote the manuscript. S.T. and A.B. performed experiments. H.T., R.U., M.F., H.G., P.L.H., and M.O. contributed to the analysis and interpretation of data and critical revisions of the manuscript for important intellectual content. All authors approved the version to be published. D.Y. and N.I. are the guarantors of this work and, as such, had full access to all the data in the study and take responsibility for the integrity of the data and the accuracy of the data analysis.

Prior Presentation. Parts of this study were presented in abstract form at the 79th Scientific Sessions of the American Diabetes Association, San Francisco, CA, 7–11 June 2019, and at the 55th European Association for the Study of Diabetes Annual Meeting, Barcelona, Spain, 16–20 September 2019. A non-peer-reviewed version of this article was posted on the bioRxiv preprint server (<https://www.biorxiv.org/content/10.1101/659904v1.full>) on 4 June 2019.

References

- Gusarova V, Alexa CA, Na E, et al. ANGPTL8/betatrophin does not control pancreatic beta cell expansion. *Cell* 2014;159:691–696
- Cox AR, Barrandon O, Cai EP, et al. Resolving discrepant findings on ANGPTL8 in β -cell proliferation: a collaborative approach to resolving the betatrophin controversy. *PLoS One* 2016;11:e0159276
- Sakaue-Sawano A, Kurokawa H, Morimura T, et al. Visualizing spatiotemporal dynamics of multicellular cell-cycle progression. *Cell* 2008;132:487–498
- Jiao Y, Le Lay J, Yu M, Naji A, Kaestner KH. Elevated mouse hepatic betatrophin expression does not increase human β -cell replication in the transplant setting. *Diabetes* 2014;63:1283–1288
- Terauchi Y, Takamoto I, Kubota N, et al. Glucokinase and IRS-2 are required for compensatory beta cell hyperplasia in response to high-fat diet-induced insulin resistance. *J Clin Invest* 2007;117:246–257
- Kim H, Toyofuku Y, Lynn FC, et al. Serotonin regulates pancreatic beta cell mass during pregnancy. *Nat Med* 2010;16:804–808
- Schraenen A, de Faudeur G, Thorrez L, et al. mRNA expression analysis of cell cycle genes in islets of pregnant mice. *Diabetologia* 2010;53:2579–2588
- Togashi Y, Shirakawa J, Orime K, et al. β -Cell proliferation after a partial pancreatectomy is independent of IRS-2 in mice. *Endocrinology* 2014;155:1643–1652
- Mort RL, Ford MJ, Sakaue-Sawano A, et al. Fucci2a: a bicistronic cell cycle reporter that allows Cre mediated tissue specific expression in mice. *Cell Cycle* 2014;13:2681–2696
- Herrera P-L, Orci L, Vassalli J-D. Two transgenic approaches to define the cell lineages in endocrine pancreas development. *Mol Cell Endocrinol* 1998;140:45–50
- Kubota SI, Takahashi K, Nishida J, et al. Whole-body profiling of cancer metastasis with single-cell resolution. *Cell Rep* 2017;20:236–250
- Alonso LC, Yokoe T, Zhang P, et al. Glucose infusion in mice: a new model to induce beta-cell replication. *Diabetes* 2007;56:1792–1801
- Porat S, Weinberg-Corem N, Tornovsky-Babaey S, et al. Control of pancreatic β cell regeneration by glucose metabolism. *Cell Metab* 2011;13:440–449
- Van de Casteele M, Cai Y, Leuckx G, Heimberg H. Mouse beta cell proliferation is inhibited by thymidine analogue labelling. *Diabetologia* 2013;56:2647–2650
- Rieck S, Kaestner KH. Expansion of beta-cell mass in response to pregnancy. *Trends Endocrinol Metab* 2010;21:151–158